*Progress In Electromagnetics Research M, Vol. 112, 29–39, 2022*

# Performance of Ultrathin Amorphous Silicon Solar Cells: An Influence of Plasmonic Effect

**Sigamani Saravanan and Raghvendra S. Dubey***

**Abstract**—Compared to crystalline silicon solar cells, thin-film solar cells are inexpensive, but a weak absorption of sunlight at a longer wavelength is a significant issue. In this perspective, an efficient light trapping mechanism is needed to facilitate the light-guiding in enhancing light absorption. This paper presents a theoretical investigation of ultrathin amorphous silicon (a-Si) solar cells using the rigorous coupled-wave analysis (RCWA) method. We noticed broadband light absorption of the designed solar cell due to an efficient light trapping geometry. Our proposed design is composed of anti-reflection coating (ITO), an absorbing layer (a-Si), a back reflector (Ag-substrate), top-indium tin oxide (ITO), and bottom-silver (Ag) nanogratings. Using an Ag-back reflector with diffraction gratings demonstrated the improved diffraction and scattering of light, which enhanced light absorption within a 50 nm thick absorbing layer. Compared to the reference solar cell, the proposed ultrathin solar cell endorsed the enhanced photovoltaic conversion, i.e., 19% and 23%, corresponding to the transverse electric (TE) and magnetic (TM) polarization conditions. Furthermore, we explore the investigations of light absorption, current density, field distributions, reflection, transmission, and parasitic losses for the optimal design of ultrathin film (a-Si) solar cells.

## 1. INTRODUCTION

Presently, monocrystalline silicon (mono-Si), polycrystalline (p-Si), and amorphous silicon (a-Si) solar cells are still dominating the photovoltaic (PV) industry due to their low cost, non-toxicity, natural abundance, and employing the advanced thin-film technology. Nevertheless, the poor light absorption in the visible and infrared spectrums is still an issue that needs to be addressed by the light-trapping mechanisms. A new optical engineering approach is required to address this shortcoming, such as textured surfaces, periodic distributed Bragg reflectors, or random nanostructures [1, 2]. The optimal design of solar cells based on metal nanoparticles or nanogratings resulted in significant scattering and diffraction of incoming light at wider angles, respectively [3, 4]. The tailored metal nanostructure improved the optical performance through plasmonic phenomena such as plasmon excitation, surface plasmon polariton (SPP), and light localization fields, all of that play a critical role in improving the photovoltaic performance [5–7].

The light-trapping mechanism in solar cells has been significantly enhanced by integrating both dielectric and metal nanogratings, which endorsed the maximal light harvesting in the absorber region by increasing the photons optical path length and lifetime [8, 9]. Shi et al. employed the finite-difference time-domain (FDTD) technique and demonstrated the design of a hybrid light-trapping structure for enhancing the efficiency of thin-film silicon solar cells. This solar cell consisted of ITO-grating on the front and Ag nanoparticles on the backside to boost the light trapping and antireflection processes. Using an optimal design of solar cell, a current density of 29.7 mA/cm$^2$ was achieved within a 1 mm thick

*Received 9 February 2022, Accepted 8 July 2022, Scheduled 24 July 2022*

* Corresponding author: Raghvendra Sarvjeet Dubey (rag_pcw@yahoo.co.in).
The authors are with the Department of Nanotechnology, Swarnandhra College of Engineering and Technology, Seetharamapuram, Narsapur, (A.P.), India.

active layer [10]. Using the rigorous coupled-wave analysis (RCWA) technique, Chao et al. studied the plasmonic thin-film solar cells under spatial dispersion. The proposed plasmonic multilayer structure (PMS) was composed of an Ag front electrode of 100 nm height, an a-Si thin active layer of 30 nm thickness, and a 500 nm thick Ag backend reflector. The designed solar cells demonstrated strongly localized surface plasmon (LSP) and surface plasmon polariton (SPP). The estimated absorbance for the silver grating was from 15 to 20%, while the absorbing region exhibited 50% [11]. Duhring et al. used the finite-element frequency-domain technique to demonstrate the broadband light absorption in a silicon thin-film solar cell. The proposed thin-film solar cell consisted of strips of Ag, Au, Al, Si, and $SiO_2$, which exhibited boosted light absorption. Due to surface plasmon resonance, they attained a higher absorption of light in a longer wavelength spectrum. Furthermore, as opposed to Ag, Au, and Al strips, the solar cell based on Si strips endorsed the four times enhanced performance [12]. Using the chemical solution technique and an extremely high-frequency plasma-enhanced chemical vapour deposition, Lai et al. fabricated hydrogenated amorphous silicon (a-Si:H) thin-film solar cells. They focused on tuning ZnO nanorods length via processing time and explored structural, optical, and morphological properties. The optimal design and fabrication process yielded an improved current density from 6.23 to 8.05 $mA/cm^2$ [13]. Mutitu et al. demonstrated the design and manufacturing of thin amorphous silicon (a-Si) solar cells with a combined dielectric-metallic back reflector. The authors demonstrated the need for more distributed Bragg reflector (DBR) layers to achieve optimum reflectance. The proposed solar cell design based on hybrid dielectric-metallic back surface reflectors explored the practical aspects of such a-Si solar cells [14]. Abass et al. investigated the optical characteristics of silicon thin-film solar cells using a dual-interface grating technology. The gratings made up of ITO and Ag were integrated at the top and bottom of the active layer of the solar cell. The dual grating structure enabled the guiding modes at a normal incidence angle. As a result, the plasmonic and photonic modes facilitated a stronger coupling of light with higher-order guided modes and resulted in the broadband absorption of the spectrum region [15]. Kumawat et al. used the finite-difference time-domain technique to design microcrystalline silicon (c-Si) solar cells. They presented the study of different plasmonic nanostructures based on nano-rings, nano-discs, nano-hemispheres, and nano-cubes integrated with the backend reflectors [16]. The performance of such plasmonic nanostructures in terms of their light absorption and current density was investigated. Eventually, nano-rings incorporated c-Si solar cells demonstrated a substantial absorption of incident light due to induced surface plasmon modes across a wide spectrum range.

Based on the literature survey, we focused on designing an optimal light trapping structure to be integrated in ultrathin silicon solar cells based on a 50 nm thick amorphous absorber layer to enhance the incident light absorption. As a result, we achieved a maximum current density of 28.3 $mA/cm^2$ and 34.3 $mA/cm^2$ for the rectangular and triangular grating based solar cells, respectively. Here, we propose a design of ultrathin amorphous silicon solar cells having an absorber layer sandwiched between the top-dielectric (ITO) and bottom-metal (Ag) nanogratings. Section 2 presents the design approach of ultrathin solar cells using the rigorous coupled-wave analysis (RCWA) technique, while the simulation findings are discussed in Section 3. Lastly, the paper is summarized in Section 4.

## 2. DESIGN APPROACH

In this work, we employed the rigorous coupled-wave analysis (RCWA) technique to design ultrathin amorphous silicon solar cells. These entire simulation processes were carried out by using Rsoft synopsis tool (DiffractMOD). This method represents the electromagnetic field as full coupled waves, and each coupled-wave is directly related to a Fourier harmonics, which allows the fully-vectorial Maxwell's equations solution under the Fourier domain. It covers a broad range of light scattering problems at horizontal periodic boundary conditions (PBC) in the $x$- and $y$-axes. Further, the diffraction efficiencies are calculated at the end of the simulation process. The incident and normalized electric-field and magnetic field vectors can be obtained by using Maxwell's equations,

$$E = \hat{u}\exp(-jk_1 \cdot r) \tag{1}$$

$$H = (j/\omega\mu_0)\nabla xE \tag{2}$$

with

$$k_1 = k_1(\sin\alpha\cos\delta\hat{x} + \sin\alpha\sin\delta\hat{y} + \cos\alpha\hat{z}) \tag{3}$$

where '$\alpha$' is the angle of incidence, and '$\delta$' is the angle betwen the plane of incidence and '$x$' axis. '$\mu_0$' is the permeability of free space, which is the assumed permeability in all the regions [17].

Figures 1(a) & 1(b) illustrate the schematic diagrams of the proposed ultrathin amorphous silicon solar cells. The proposed solar cell was composed of an anti-reflection coating of ITO with its thickness of 90 nm ($T_{\mathrm{ARC}}$), an absorber ($T_c$, a-Si) layer of 50 nm, an 'Ag' back reflector ($T_{\mathrm{BR}}$) of a thickness of 200 nm, the ITO dielectric nanogratings ($Gt$) of thickness 20 nm, grating duty cycle ($G_{\mathrm{dc}} = 0.5$), grating period ($Gp = 600$ nm), and an 'Ag' metal nanograting ($Gt$) with its thickness of 20 nm. Figures 1(a) & 1(b) illustrate the rectangular and triangular Ag gratings-based designs of ultrathin silicon solar cells, respectively. The top (ITO) gratings exhibited increased light absorption in the wavelength range 492–455 nm and 577–492 nm.

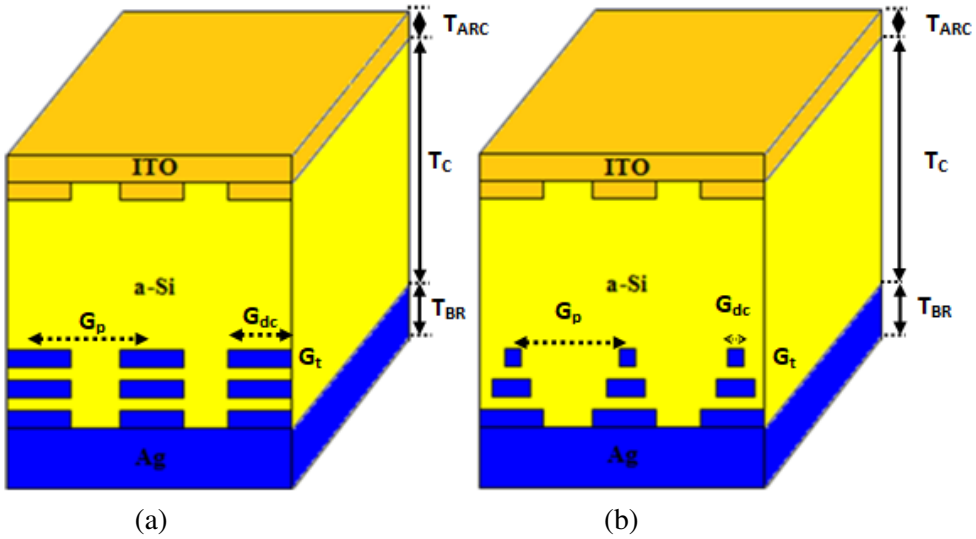


**Figure 1.** Schematic designs of proposed (a) rectangular and (b) triangular gratings based on ultrathin a-Si solar cells.

Similarly, metal (Ag) gratings demonstrated a higher light absorption in the longer wavelength region, which could be due to the scattering of incoming light resulting from excitation of localized surface plasmons (LSP) influenced by the size and surrounding medium of the gratings. The use of gratings maximized the absorption of light in amorphous silicon. In a similar way, Guo et al. explored the increased broadband light absorption in the proposed solar cell due to the usage of hybrid top-ITO and bottom-Si/Ag gratings [18]. In this work, Maxwell's equations and Fourier harmonics were analyzed by using the RCWA technique, often known as the simple approach. At a normal incident angle, the irradiated plane wave was in the wavelength range from 300 to 1200 nm. The perfect boundary condition (PBC) was used at the left and right ($x, y$-axis) boundaries, while the perfect match layer (PML) was applied at the top and bottom of the solar cell. The PBC stipulates that the field can leave boundary from one side of the domain and allows reenter in the domain on the opposite side. The PML boundary is highly lossy used to avoid unwanted reflection from the incident light.

## 3. RESULTS & DISCUSSION

Figures 2(a) and 2(b) show the optical absorption and current density of the proposed design of ultrathin amorphous silicon solar cells, respectively. As shown in Figure 2(a), the symmetrical 'Ag' grating-based solar cell exhibited an optimum absorption throughout the whole solar spectrum, whereas the triangular 'Ag' grating-based solar cell exhibited a significant light absorption in the longer wavelengths region. This improvement can be ascribed to the light scattering and guided-mode processes.

The triangular 'Ag' gratings enabled increased light absorption in the absorber region due to the coupling of incoming light, which induced the plasmonic and photonic modes [19–21]. As will be described later, it is seen that the photonic mode was dominant in the transverse electric (TE)

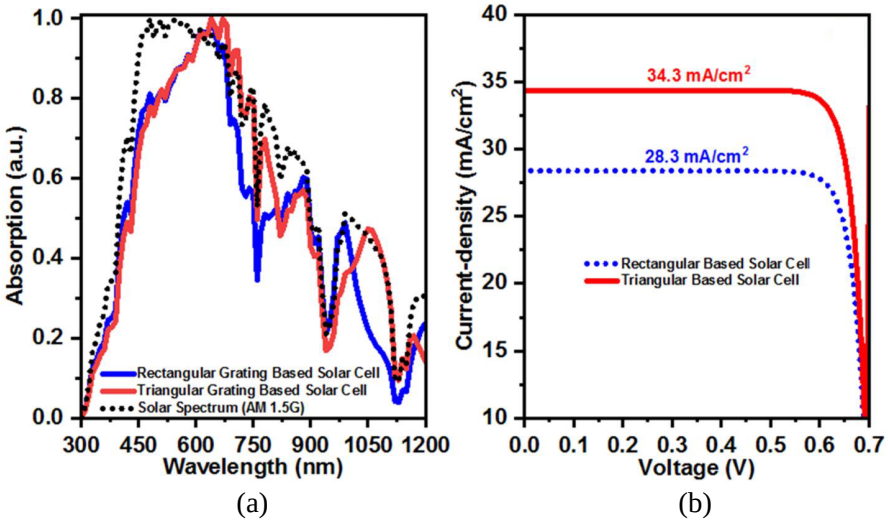


**Figure 2.** (a) Optical absorption spectrum and (b) current density vs voltage of rectangular and triangular gratings based ultrathin a-Si solar cells.

polarization case, while the plasmonic mode was dominant in the transverse magnetic (TM) polarization case. Figure 2(b) shows the current density (Jsc) versus voltage plot of the rectangular and triangular grating-based ultrathin a-Si solar cells. The bottom-Ag triangular and top-ITO dielectric gratings played a significant role in the proposed solar cell design. The plasmonic solar cell reduces parasitic absorption using silver gratings, while the field distribution shows their significant impact. The obtained maximal current densities were 28.4 mA/cm$^2$ and 34.4 mA/cm$^2$ for the rectangular and triangular gratings based solar cells, respectively. The enhanced current density in the ultrathin absorber layer is remarkable for later solar cells. The amorphous silicon demonstrated enhanced absorption due to strong field-localization, scattering, and diffraction enhanced near the metal-semiconductor material interface [22–24]. The metallic (Ag) nanostructure was promising due to increased resonant modes and exciton lifetime [25–27]. In a similar report, Abass et al. studied the amorphous silicon solar cells with dual (ITO and Ag) gratings in which top ITO grating facilitated the guiding of the incident light, including in the shorter and longer wavelength regions [15]. We have compared the performance of the proposed solar cell with the reported ones, as shown in Table 1.

**Table 1.** Performance comparison of various thin-film silicon solar cells.

| S.N. | Solar Cells | Absorber Layer Thickness | Current Density (mA/cm$^2$) | Cell Efficiency (%) | Ref. |
|---|---|---|---|---|---|
| 1 | Silicon | 1 µm | 29.7 | - | [10] |
| 2 | Amorphous Silicon | 400 nm | 8.05 | 4.51 | [13] |
| 3 | Amorphous Silicon | 500 nm | 25.6 | - | [14] |
| 4 | Crystalline Silicon | - | 21.66 | - | [28] |
| 5 | Tandem (Perovskite/Silicon) | 430 nm | 19.9 | 24.7 | [29] |
| 6 | Crystalline Silicon | 1.5 µm | 18.87 | - | [30] |
| 7 | Amorphous silicon | 50 nm | 34.3 | 23 | Present work |

Comparatively, the present work evidenced the outstanding performance of the solar cell with its current density of 34.3 mA/cm$^2$ and cell efficiency of 23%.

Figure 3 depicts the comparison of cell efficiencies ($\eta$%) of the proposed ultrathin amorphous silicon solar cells for transverse electric (TE) and magnetic (TM) polarization conditions. The reference solar cell without top and bottom gratings showed its cell efficiency of 6%, whereas the proposed dual grating-based solar cell demonstrated enhanced efficiency for both the TM and TE polarization cases. For the TM case, the rectangular grating-based solar cell demonstrated its efficiency of 19%, while it was 23% for the solar cell based on triangular gratings. Similarly, the cell efficiencies were 19% and 20% for the TE case, corresponding to the solar cells based on rectangular and triangular gratings. Compared to various solar cells, we noticed an open-circuit voltage of 0.7 V, fill factor of 84.58%, and current density of 34.3 mA/cm$^2$ using a 50 nm thick absorber layer.

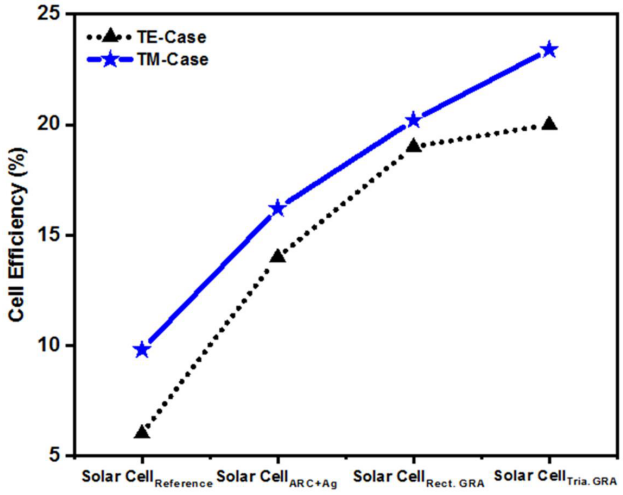


**Figure 3.** Photovoltaic performance of various solar cells for TE and TM polarization cases.

Figure 4 shows the magnetic field distribution in the rectangular solar cell at various incident wavelengths corresponding to the absorption curve (dotted-green curve) as shown in Figure 2(a). Figures 4(a) & 4(b) demonstrate the overlapped resonant modes at 641 and 701 nm wavelength. Comparatively, Figure 4(b) exhibits a strong field with more field resonance modes between the dielectric and metal gratings (yellow color). Figure 4(c) illustrates how scattering and guided modes increased photon absorption. When the incident wavelength is increased, the field intensity becomes high and exhibits enhanced absorption, as shown in Figure 4(d).

Figure 5 depicts the magnetic field distribution in the longer wavelength range. In general, thin-film silicon solar cells have weak absorption in the infrared spectrum. In this view, our proposed design exhibits prominent peaks in the infrared spectrum, as depicted in Figure 2(a). This improvement can be attributed to the integrated metal nanogratings, as shown in Figures 5(a)–5(d).

In a similar way, Wang et al. claimed a significant role of bottom metal grating in the generation of guided modes to overcome the problem of weak light absorption [31]. Figures 6(a)–6(d) demonstrate the strong field confinement in the absorber layer for the solar cell based on triangular metal gratings due to the coupling of incident light into surface-guiding and localized modes. The field profile demonstrates a strong field distribution due to the triangular metal nanogratings. Thus, the interaction of light with the material extends the photon path length inside the absorber, enhancing optical harvesting [32]. We can notice the distinct field distribution profile at various wavelengths indicating the characteristics of the plasmonic and photonic modes. The grating width *(Gw)* was determined using the straightforward formula $Gw = Gp * Gdc$. The grating period *(Gp)* was 500 nm, with a duty cycle *(Gdc)* of about 550 nm. Likewise, the grating thickness *(Gt)* and the distance between the gratings ($D = Gt$) were both maintained the same (20 nm).

Figure 6(a) shows the field distribution profile at wavelength 641 nm. Here, one can notice the localized surface plasmon (LSP) on the metal grating, while field-excitation and surface plasmon-

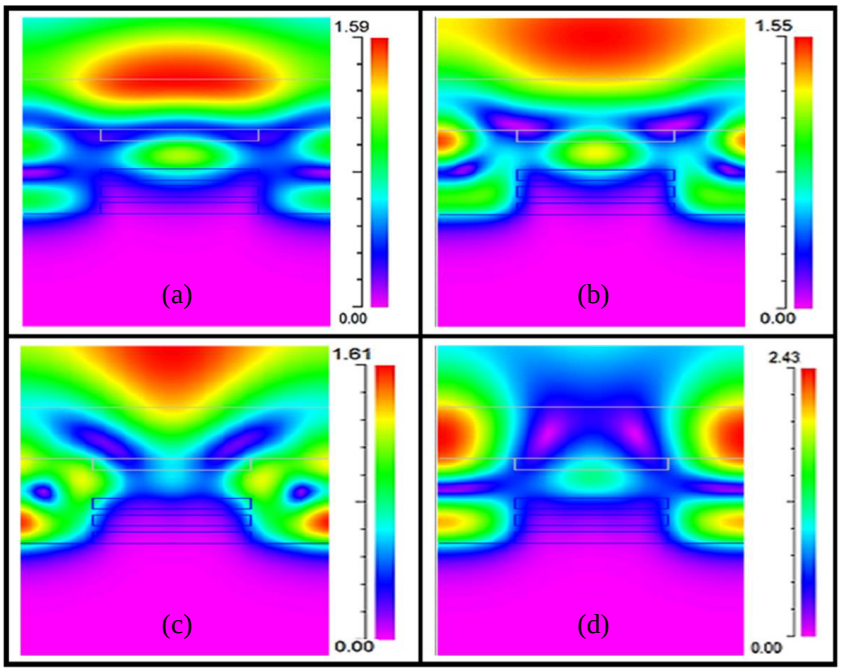


**Figure 4.** Magnetic field distribution in solar cell based on rectangular gratings at wavelengths (a) 641 nm, (b) 701 nm, (c) 741 nm and (d) 809 nm.

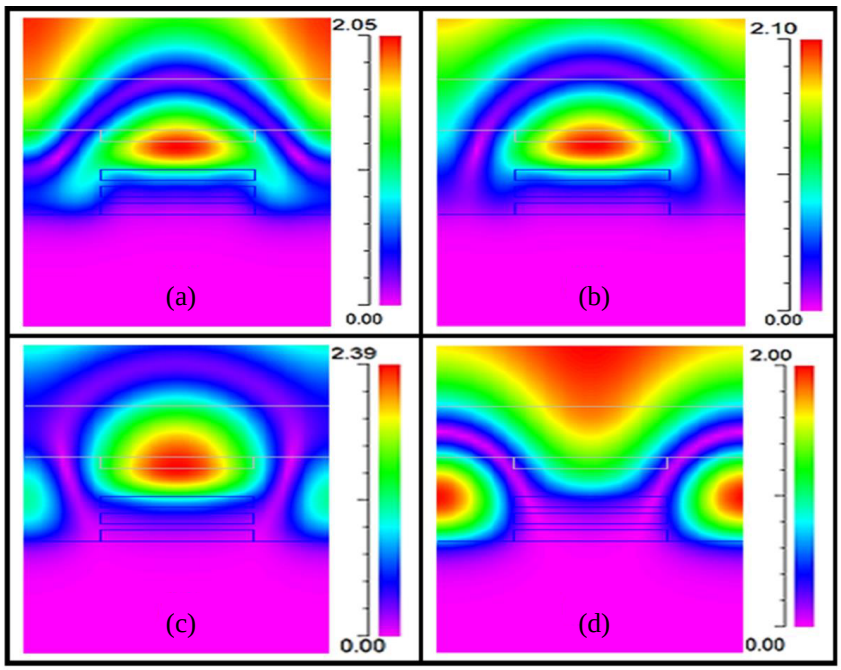


**Figure 5.** Magnetic field distribution in solar cell based on rectangular gratings at wavelengths (a) 882 nm, (b) 920 nm, (c) 991 nm and (d) 1200 nm.

polariton (SPP) are in the absorber region. In a similar way, we can observe a strong plasmonic effect as shown in Figures 6(b) and 6(c) as compared to the previous one. The photonic mode assisted the waveguiding of the electromagnetic waves, whereas the plasmonic mode generated the localized

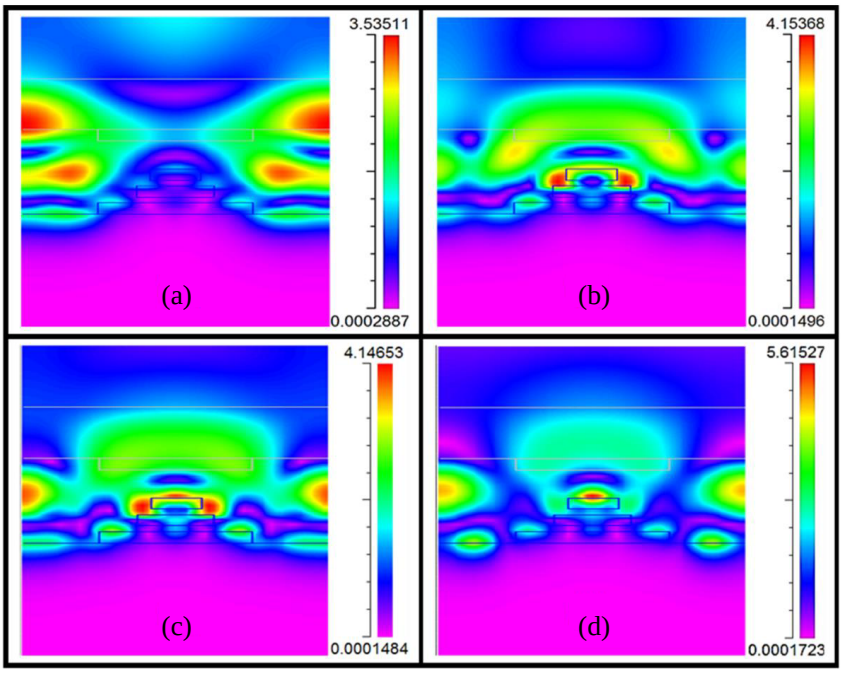


**Figure 6.** Magnetic field distribution in solar cell based on triangular gratings at wavelengths (a) 641 nm, (b) 711 nm, (c) 741 nm and (d) 782 nm.

surface plasmons indicating the oscillation of free electrons coupled and guided towards the collector side. This resulted in the enhancement of solar cell efficiency. Figure 6(d) endorsed the LSP and surface excitation at wavelength 782 nm. If we compare Figures 6(a)–6(d), an enhancement in field distribution is noticeable. The excitation of surface plasmon modes in the proposed triangular grating-based solar cell can be ascribed to the interaction among the free electrons in the metal grating and electromagnetic waves. This design approach enables a larger scattering angle and increases the optical path length of the photons inside the semiconductor/absorber region. As a result, increased light absorption was stimulated owing to the induced surface plasmons. In this way, an optimal design of solar cell geometry can felicitate the generation of plasmonic effect to enhance the solar absorption spectrum.

We know that the surface plasmon modes follow dispersion relations at the interface between metal and dielectric [33, 34]. Here, the surface plasmon (SP) effect includes the contribution of surface plasmon-polariton (SPP) and localized surface plasmon (LSP).

Figures 7(a)–(d) show the magnetic field distribution in longer wavelengths (i.e., 882, 920, 1050, and 1170 nm). The localization of the magnetic field with an excited state can be noticed on the metal grating and the interface between the metal and dielectric layer for the case of excitation wavelength 882 nm, as shown in Figure 7(a). At a higher excitation wavelength of 920 nm, as shown in Figure 7(b), one can observe the field enhancement near the bottom grating edges and in-between the neighboring gratings.

This was found associated with the Fabry-Perot surface plasmon polariton and surface plasmons in metal (Ag) and dielectric (ITO) interface, which reflects light front and back of the neighboring gratings [35]. Referring to Figure 2(a), one can notice the enhanced absorption at wavelength 1050 nm. Here, Figure 7(c) depicts the magnetic field profile at an excitation wavelength of 1050 nm, which evidenced the strong field intensity at the nanogratings due to the strong localized surface plasmon. Figure 7(d) endorsed the distinct field distribution, which is significant in improving the solar cell's performance. This corresponds to the bottom surface-excitation (metal and dielectric interface) and localized-surface plasmon on the gratings.

We have studied the optical absorption and parasitic losses associated with the proposed solar cell design based on top rectangular and bottom triangular grating. In our design, each component played

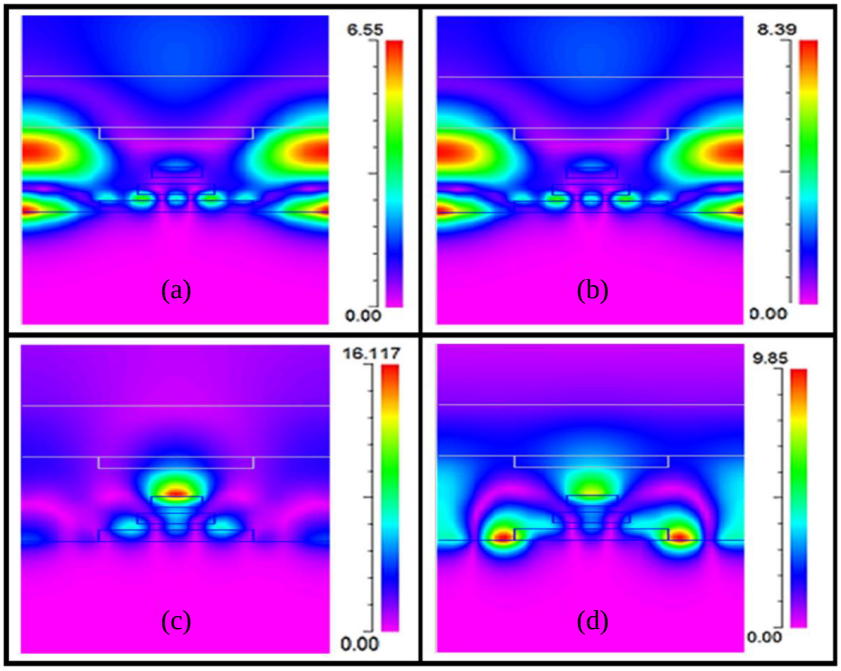


**Figure 7.** Magnetic field distribution in solar cell based on triangular gratings at wavelengths (a) 882 nm, (b) 920 nm, (c) 1050 nm and (d) 1170 nm.

a significant role. For example, the anti-reflection coating (ARC) layer significantly enhanced light in the absorbing layer by diffusing the light in the device.

The top dielectric grating facilitated the guiding of light by prolonging its path length via the induced photonic mode, while the bottom metal grating induced the plasmonic mode. In this way, it all together improved the performance of the solar cell. An optimal design of solar cells is very important to reduce the loss of solar light and, therefore, enhance light absorption. In this view, we have studied the absorption and parasitic losses in each layer of the solar cell under the total incident photon flux of the AM1.5 spectrum between 300 and 1200 nm.

Figure 8 illustrates the analysis of the various losses associated with the proposed design of the solar cell. The proposed solar cell was composed of a 50 nm ultrathin amorphous silicon absorber integrated with the top dielectric and bottom metal gratings which evidenced the predominant effect of induced photonic and plasmonic modes. Overall, optical absorption in the devices was 63%, including 4% in the anti-reflective layer, 7% in top-dielectric gratings, 29% in bottom metal gratings, and 23% in the remaining active region. We could also estimate the reflection loss of 24% with 13% parasitic loss due to the back metal layer. The metal back layer showed the parasitic absorption losses due to the charge recombination.

We have compared the proposed solar cell design with the reference solar cell without the top-dielectric and bottom-metal gratings. A significant absorption enhancement can be noticed compared with the reference cell, as illustrated in Figure 9, which shows the optical absorption of the reference solar cell (green curve) and ultrathin amorphous silicon solar cell (blue curve). The reference cell yielded the absorption as much as 21.1%, while that of our proposed ultrathin solar cell was about 74.1%.

Remarkably, the triangular metal grating-based solar cell could yield about three times enhanced light absorption due to the efficient light trapping mechanism sustained through the induction of photonic and plasmonic modes. The optimal design of ultra-thin solar cells showed multi-resonant absorption in the wavelength range from 450 nm to 1200 nm. Notably, an overall enhancement in light absorption is noticeable in the longer wavelength region, as shown in Figure 9. Overall, our simulated results demonstrated the extraordinary performance of the proposed ultrathin a-Si solar cells due to the integrated dielectric and metal gratings. In this study, we designed and demonstrated the rectangular and triangular gratings based on ultrathin amorphous silicon solar cells; however, later, one evidenced

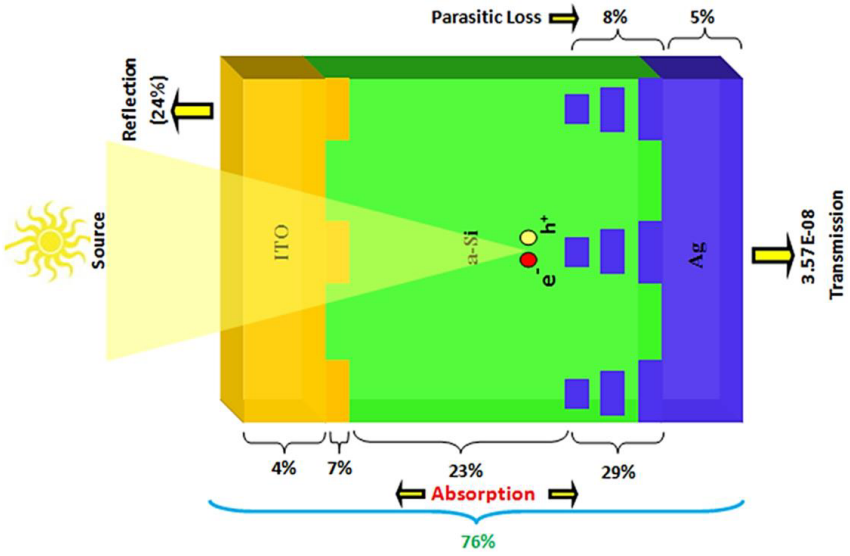


**Figure 8.** An illustration of absorption and parasitic losses in the different layers of ultrathin a-Si solar cell.

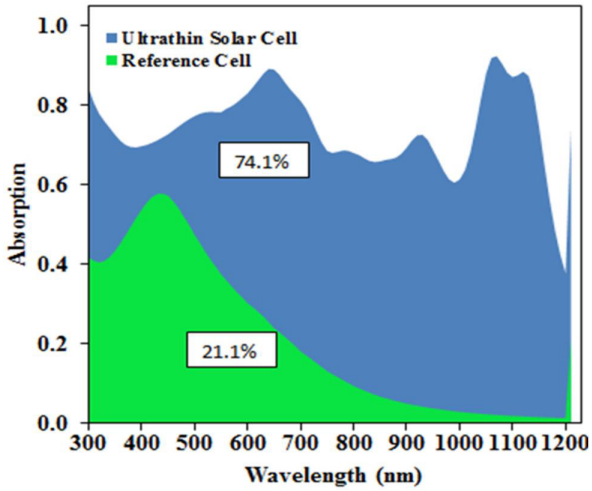


**Figure 9.** Light absorption comparison of reference and proposed ultrathin a-Si solar cell.

the broader light absorption due to the induced photonic (for guiding the light) and plasmonic modes. The practical aspect of the proposed solar cell is challenging; however, the nano-imprinting technique and advanced fabrication technology such as plasma-enhanced chemical vapor deposition and electron-beam lithography techniques could be the available resources for fabricating such ultrathin amorphous silicon solar cells.

## 4. CONCLUSIONS

We proposed the design and simulation of two different 50 nm ultrathin amorphous silicon solar cells integrated with top-dielectric and bottom-metal nanogratings. The RCWA method was employed to study the photovoltaic performance of the solar cells based on rectangular and triangular nanogratings at the bottom. The highest cell efficiency was 23% for the transverse magnetic (TM) polarization condition from the ultrathin a-Si solar cell based on bottom-triangular nanogratings. Top-ITO nanogratings illustrated the improved light absorption in the shorter spectral region, while the bottom-

silver nanogratings yielded broad absorption in the longer wavelength range. This enhancement of light absorption could be correlated to the induction of photonic mode, which supported the guiding mechanism of incident light crossing the anti-reflective coating. The plasmonic mode induced the surface plasmons at the interface of silver nanogratigs and semiconductors. To sum up, this solar cell design is challenging for its experimental realization but feasible with modern fabrication technology with the compromised manufacturing cost. The proposed solar cell design is promising for its terrestrial and space applications.

## DATA AVAILABILITY

The authors confirm that the related data is available in the manuscript. The raw supporting findings are available upon reasonable request to the corresponding author.

## REFERENCES

1. Venkatesh, Y., R. S. Dubey, and B. Kumar, "Rapid and economic fabrication approach of dielectric reflectors for energy harvesting applications," *Scientific Reports*, Vol. 10, 15930-1–9, 2020.
2. Saravanan, S. and R. S. Dubey, "Study of ultrathin-film amorphous silicon solar cell performance using photonic and plasmonic nanostructure," *International Journal of Energy Research*, 1–9, 2021.
3. Saravanan, S. and R. S. Dubey, "Optical absorption enhancement in 40 nm ultrathin film silicon solar cells assisted by photonic and plasmonic modes," *Optics Communications*, Vol. 377, 65–69, 2016.
4. Sidharthan, R. and V. M. Murukeshan, "Improved light absorption in thin film solar cell using combination of gap modes and grating back reflector," *Thin Solid Films*, 581–584, 2013.
5. Olaimat, M. M., L. Yousefi, and O. M. Ramahi, "Using plasmonics and nanoparticles to enhance the efficiency of solar cells: Review of latest technologies," *Journal of the Optical Society of America B*, Vol. 38, No. 2, 638–651, 2021.
6. Aly, A. M. A., M. Hussein, A. Yahia, M. F. O. Hameed, and S. S. A. Obayya, "Highly efficient $SiO_2$ trapezoidal grating-based thin-film solar cell," *Journal of the Optical Society of America B*, Vol. 38, No. 3, 922–931, 2021.
7. Du, J., Y. An, C. Zhu, X. Li, and D. Ma, "Photonic design and electrical evaluation of dual-functional solar cells for energy conversion and display applications," *Nanoscale Research Letters*, Vol. 14, 1–9, 2019.
8. Subhan, F. E., A. D. Khan, F. E. Hilal, A. D. Khan, S. D. Khan, R. Ullah, M. Imran, and M. Noman, "Efficient broadband light absorption in thin-film a-Si solar cell based on double sided hybrid bi-metallic nanogratings," *RSC Advances*, Vol. 10, 11836–11842, 2020.
9. Amalathas, A. P. and M. M. Alkaisi, "Nanostructures for light trapping in thin film solar cells," *Micromachines*, Vol. 10, No. 619, 1–18, 2019.
10. Shi, Y., X. Wang, W. Liu, T. Yang, and F. Yang, "Hybrid light trapping structures in thin film silicon solar cells," *Journal of Optics*, Vol. 16, 075706-1–7, 2014.
11. Chao, C. C., C. M. Wang, and J. Y. Chang, "Spatial distribution of absorption in plasmonic thin film solar cells," *Optics Express*, Vol. 18, No. 11, 11763–11771, 2010.
12. Duhring, M. B., N. A. Mortensen, and O. Sigmund, "Plasmonic versus dielectric enhancement in thin film solar cells," *Applied Physics Letters*, Vol. 100, 211914-1–4, 2012.
13. Lai, F. I., J. F. Yang, Y. C. Hsu, and S. Y. Kuo, "Improvement of amorphous silicon thin-film photovoltaic cells with zinc oxide nanorods," *Crystals*, Vol. 10, 1124-1–10, 2020.
14. Mutitu, J. G., S. Shi, A. Barnett, and D. W. Prather, "Hybrid dielectric-metallic back reflector for amorphous silicon solar cells," *Energies*, Vol. 3, 1914–1933, 2010.
15. Abass, A., K. Q. Le, A. Alu, M. Burgelman, and B. Maes, "Dual interface gratings for broadband absorption enhancement in thin film solar cells," *Physics Review B*, Vol. 85, 115449-1–7, 2012.
16. Kumawat, U. K., K. Kumar, S. Mishra, and A. Dhawan "Plasmonic enhanced microcrystalline silicon solar cells," *Journal of the Optical Society of America B*, Vol. 37, No. 2, 495–504, 2020.

17. Moharam, M. G. and T. K. Gaylord, "Three-dimensional vector coupled-wave analysis of planar-grating diffraction," *Journal of the Optical Society of America*, Vol. 73, No. 9, 1105, 1983.
18. Guo, X., J. Liu, and S. Zhang, "Design of light trapping structures for ultrathin solar cells," *Photonics and Optoelectronics (P&O)*, Vol. 3, 66–69, 2014.
19. Ferry, V. E., J. N. Munday, and H. A. Atwater, "Design considerations for plasmonic photovoltaics," *Advanced Materials (Deerfield Beach Fla.)*, Vol. 22, No. 43, 4794–4808, 2010.
20. Pala, R. A., J. White, E. Barnard, J. Liu, and M. L. Brongersma, "Design of plasmonic thin-film solar cells with broadband absorption enhancements," *Advanced Materials (Deerfield Beach Fla.)*, Vol. 21, No. 34, 3504–3509, 2009.
21. Panoiu, N. C. and R. M. Osgood, Jr., "Enhanced optical absorption for photovoltaics via excitation of waveguide and plasmon-polariton modes," *Optics Letters*, Vol. 32, No. 19, 2825–2827, 2007.
22. Pahud, C., V. Savu, M. Klein, O. Vazquez-Mena, F.-J. Haug, J. Brugger, and C. Ballif, "Stencil-nanopatterned back reflectors for thin-film amorphous silicon n-i-p solar cells," *IEEE Journal of Photovoltaics*, Vol. 3, No. 1, 22–26, 2013.
23. Zilio, P., D. Sammito, G. Zacco, M. Mazzeo, G. Gigli, and F. Romanato, "Light absorption enhancement in heterostructure organic solar cells through the integration of 1-D plasmonic gratings," *Optics Express*, Vol. 20, No. S4, A476–A488, 2012.
24. Dunbar, R. B., T. P. Fadler, and L. Schmidt-Mende, "Highly absorbing solar cells — A survey of plasmonic nanostructures," *Optics Express*, Vol. 20, No. S2, A177–A189, 2012.
25. Lee, S. and S. Kim, "Optical absorption characteristic in thin a-Si film embedded between an ultrathin metal grating and a metal reflector," *IEEE Photonics*, Vol. 5, No. 5, 2013.
26. Villa, F., T. Lopez-Rios, and L. E. Regalado, "Electromagnetic modes in metal-insulator-metal structures," *Physics Review B, Condensed Matter*, Vol. 63, No. 16, 165103-1–165103-4, 2001.
27. Vuong, L. T., G. Kozyreff, R. Betancur, and J. Martorell, "Cavity-controlled radiative recombination of excitons in thin-film solar cells," *Applied Physics Letters*, Vol. 95, No. 23, 233106-1–233106-3, 2009.
28. Chen, K., N. Zheng, S. Wu, J. He, Y. Yu, and H. Zheng, "Effective light trapping in c-Si thin-film solar cells with a dual-layer split grating," *Appl. Opt.*, Vol. 60, No. 33, 10312–10321, 2021.
29. Tennyson, E. M., K. Frohna, W. K. Drake, F. Sahli, T. C.-J. Yang, F. Fu, J. Werner, C. Chosy, A. R. Bowman, T. A. S. Doherty, Q. Jeangros, C. Ballif, and S. D. Stranks, "Multimodel microscale imaging of textured perovskite-silicon tandem solar cells," *ACS Energy Letters*, Vol. 6, No. 6, 2293–2304, 2021.
30. Dubey, R. S. and S. Saravanan, "Impact of distributed Bragg's reflectors and nanogratings in thin film silicon solar cells," *Nanosyst: Phys. Chem. Math.*, Vol. 13, No. 2, 223–229, 2022.
31. Wang, W., S. Wu, K. Reinhardt, Y. Lu, and S. Chen, "Broadband light absorption enhancement in thin-film silicon solar cells," *Nano Letters*, Vol. 10, No. 6, 2012–2018, 2010.
32. Khaleque, T. and R. Magnusson, "Light management through guided-mode resonances in thin-film silicon solar cells," *Journal of Nanophotonics*, Vol. 8, 083995-1–13, 2014.
33. Barnes, W. L., A. Dereux, and T. W. Ebbesen, "Surface plasmon subwavelength optics," *Nature*, Vol. 424, No. 6950, 824–830, 2003.
34. Zhu, L.-H., M.-R. Shao, R.-W. Peng, R.-H. Fan, X.-R. Huang, and M. Wang, "Broadband absorption and efficiency enhancement of an ultra-thin silicon solar cell with a plasmonic fractal," *Optics Express*, Vol. 21, No. S3, A313–A323, 2013.
35. Lee, S., S. J. In, D. R. Mason, and N. Park, "Incorporation of nanovoids into metallic gratings for broadband plasmonic organic solar cells," *Optics Express*, Vol. 21, No. 4, 4055–4060, 2013.